

The Josephson critical current in a long mesoscopic S-N-S junction

P. Dubos, H. Courtois, B. Pannetier

Centre de Recherches sur les Très Basses Températures-C.N.R.S. associated to Université Joseph Fourier, 25 Ave. des Martyrs, 38042 Grenoble, France

F. K. Wilhelm,^{1,2} A. D. Zaikin³ and G. Schön¹

¹*Institut für Theoretische Festkörperphysik, Universität Karlsruhe, 76128 Karlsruhe, Germany*

²*Quantum Transport Group, Department of Applied Physics and DIMES, TU Delft, 2600 GA Delft, The Netherlands*

³*Forschungszentrum Karlsruhe, Institut für Nanotechnologie, 76021 Karlsruhe, Germany*

(November 26, 2024)

We carry out an extensive experimental and theoretical study of the Josephson effect in S-N-S junctions made of a diffusive normal metal (N) embedded between two superconducting electrodes (S). Our experiments are performed on Nb-Cu-Nb junctions with highly-transparent interfaces. We give the predictions of the quasiclassical theory in various regimes on a precise and quantitative level. We describe the crossover between the short and the long junction regimes and provide the temperature dependence of the critical current using dimensionless units $eR_N I_c / \epsilon_c$ and $k_B T / \epsilon_c$ where ϵ_c is the Thouless energy. Experimental and theoretical results are in excellent quantitative agreement.

73.23.Ps, 74.50.+r, 74.80.Fp, 85.30St

The Josephson effect is well known to exist in weak links connecting two superconducting electrodes S, e.g. a tunnel barrier I, a short constriction C or a normal metal N (S-I-S, S-C-S and S-N-S junctions). This effect manifests itself in a non-dissipative DC-current flowing through the Josephson junction at zero voltage. At weak coupling, e.g. in the S-I-S case, the Josephson current can be expressed as $I_s = I_c \sin \varphi$ where φ is the phase difference between the two superconducting condensates and the maximum supercurrent I_c is called the critical current.

The Josephson effect in S-N-S junctions has been studied in a variety of configurations. The early experiments of Clarke¹ and Shepherd² were performed in Pb-Cu-Pb sandwiches. In these experiments and in the pioneering calculations by de Gennes,³ it was already realized that the presence of a supercurrent in such structures is due to the proximity effect. It can be understood as the generation of superconducting correlations in a normal metal connected to a superconductor, mediated by phase-coherent Andreev reflections at the S-N interface. The critical current I_c is limited by the “bottleneck” in the center of the N-layer, where the pair amplitude is exponentially small, $I_c \propto e^{-L/L_T}$. Here $L_T = \sqrt{\hbar D / 2\pi k_B T}$ is the characteristic thermal length in the diffusive limit and L is the length of the junction. These calculations, as well as those by Fink,⁴ analyzed the temperature dependence of I_c within the Ginzburg-Landau theory in the vicinity of the superconducting critical temperature T_c . Later, the critical current of diffusive S-N-S microbridges^{5,6} was successfully described by Likharev⁷ with the aid of the quasiclassical Usadel equations.⁸ In this work, the emphasis was put on the high temperature regime where the superconducting order parameter is smaller than the thermal energy $\Delta \ll k_B T$. A more general study of the Josephson effect in diffusive S-N-S junctions was made in

Ref. 9.

More recently, experimental data on long Josephson junctions¹⁰ showed a surprising temperature-dependence, which turned out to be in a strong disagreement with the early theory by de Gennes. These data have been discussed by some of us¹¹ within the quasiclassical approach which we will also use in the present work. Fink¹² attempted to analyze the data¹⁰ by means of an extrapolation of the Ginzburg-Landau theory to low temperatures.

The proximity effect in mesoscopic hybrid structures consisting of normal and superconducting metals attracted a growing interest during the recent years.¹³ Here we will consider mesoscopic diffusive S-N-S junctions where the sample length is much larger than the elastic mean free path l_e but smaller than the dephasing length L_ϕ : $l_e < L < L_\phi$. In N-S junctions and Andreev interferometers, we can identify – both theoretically and experimentally – the natural energy scale for the proximity effect.^{14,15} It is given by the Thouless energy $\epsilon_c = \hbar D / L^2$. Here $D = v_F l_e / 3$ is the diffusion constant of the N-metal, v_F is the Fermi velocity. In contrast to the energy gap Δ which is set by the interactions in the superconducting electrodes, the energy scale ϵ_c is a single-electron quantity: ϵ_c / \hbar is merely the diffusion rate across the sample for a single electron. This energy scale remains important in non-equilibrium situations, e.g. if one drives the supercurrent across a S-N-S junction by the injection of a control current in the N-metal.^{16–18}

The main purpose of the present paper is to carry out a detailed experimental investigation of the equilibrium supercurrent in relatively long diffusive S-N-S junctions with highly transparent N-S interfaces as well as a quantitative comparison of our data to the theoretical predictions. Here, a long junction means that the junction length L is much bigger than $\sqrt{\hbar D / \Delta}$. This is equivalent

to $\Delta \gg \epsilon_c$. In order to perform this comparison at all relevant temperatures, we complete the previous studies by providing a rigorous expression for the Josephson critical current at $T \rightarrow 0$ which was not properly evaluated before. Our experimental results are in excellent agreement with the theoretical predictions.

As before,^{9,11} our theoretical approach is based on the quasiclassical Green's functions in imaginary time. The proximity effect is described by a finite pair amplitude F in the N-metal (see [19] and references therein). We will assume N-S interfaces to be fully transparent and neglect the suppression of the pair potential Δ in the S electrodes near the N-S interface. This is appropriate at $T \ll T_c$ or if the reservoirs are very massive as compared to the normal metal. Within those bounds, our calculation does not contain further approximations and is e.g. valid at arbitrary temperature and sample size. We will now proceed by discussing certain limits.

In the high temperature regime $k_B T \gg \epsilon_c$ (or, equivalently, $L \gg L_T$), the solution is well known. In this case the mutual influence of the two superconducting electrodes can be neglected and the Usadel equations can be linearized in the N-metal, except in the vicinity of the N-S interfaces. One finds :⁹

$$eR_N I_c = 64\pi k_B T \sum_{n=0}^{\infty} \frac{L}{L\omega_n} \frac{\Delta^2 \exp(-L/L\omega_n)}{(\omega_n + \Omega_n + \sqrt{2(\Omega_n^2 + \omega_n^2)})^2} \quad (1)$$

where R_N is the N-metal resistance, $\omega_n = (2n+1)\pi k_B T$ is the Matsubara frequency, $\Omega_n = \sqrt{\Delta^2 + \omega_n^2}$ and $L\omega_n = \sqrt{\hbar D/2\omega_n}$. If T is close to the critical temperature of S, the gap is small as compared to the thermal energy : $\Delta \ll k_B T$. In this limit, Eq. (1) coincides with the result derived by Likharev.⁷

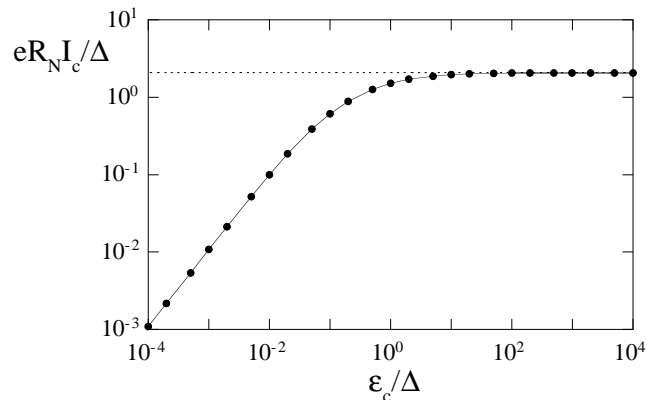


FIG. 1. Calculated dependence of the zero temperature $eR_N I_c$ product in units of Δ as a function of the ratio ϵ_c/Δ . I_c is the Josephson critical current, R_N the normal state resistance, ϵ_c is the Thouless energy and Δ is the superconducting gap of S. The long junction regime is on the left part of the graph where $\epsilon_c < \Delta$, the short junction regime is on the right part where $\epsilon_c > \Delta$. The dashed line corresponds to the Kulk-Omel'yanchuk formula²⁵ at $T = 0$.

At lower temperatures $k_B T \lesssim \epsilon_c$ evaluation of I_c involves solutions of the Usadel equation at *all* energies¹⁹. In order to determine the precise value²¹ of the critical current, we performed a numerical solution of the Usadel equations for the whole range of Matsubara frequencies. In the long junction limit ($\Delta \gg \epsilon_c$), the zero-temperature $eR_N I_c$ is found to be proportional to ϵ_c :

$$eR_N I_c(T = 0) = 10.82\epsilon_c. \quad (2)$$

In this case, the current phase relation is slightly different from a sine and the supercurrent maximum occurs at $\varphi = 1.27\pi/2$. As compared to previous estimates,^{11,12} the exact numerical prefactor in this formula turns out to be unexpectedly high. This observation is crucial for a quantitative comparison between theory and experiment not only in the case of conventional junctions but also for high- T_c S-N-S junctions²⁰ or devices involving carbon nanotubes.²²

Let us now turn to the short junction regime $\Delta \ll \epsilon_c$, i.e. to the case of dirty S-C-S weak links described in Ref. 25,26. Our numerical results reproduces quantitatively the behaviours of both the current-phase relation and the zero-temperature critical current : $eR_N I_c \approx 1.326\pi\Delta/2$ at $\varphi = 1.25\pi/2$.^{25,26} This results confirms the precision of our calculation in describing both the long junction and the short junction regimes. Our numerical results for $I_c(T = 0)$ as a function of the Thouless energy ϵ_c are presented in Fig. 1. It confirms that it is the minimum of the gap Δ and the Thouless energy ϵ_c which limits the critical current in diffusive S-N-S junctions. At $\epsilon_c \simeq \Delta$, the critical current value remains close to the short junction case.

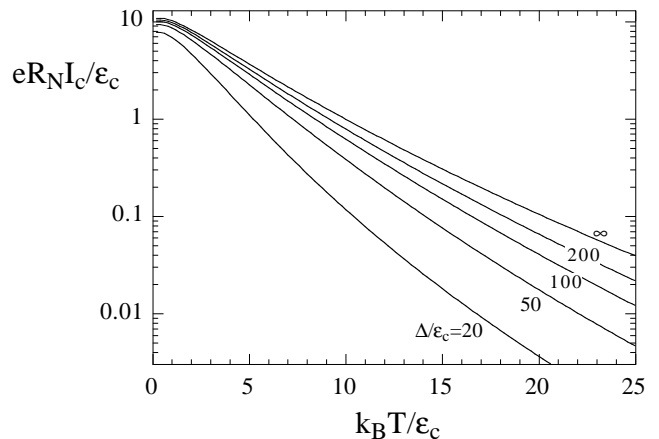


FIG. 2. Calculated temperature dependence of the $eR_N I_c$ product. The different curves correspond to various values of the ratio Δ/ϵ_c in the long junction regime. The curve for $\Delta/\epsilon_c \rightarrow \infty$ is universal in the sense it does not depend on Δ . Note that $k_B T/\epsilon_c = L^2/2\pi L_T^2$.

In the following, we will focus on long junctions $\Delta > \epsilon_c$. Fig. 2 shows the temperature dependence of the $eR_N I_c$ product for various values of the superconducting gap in the long junction regime. Both axis are given in

units of the Thouless energy. The low-temperature part ($k_B T < 5\epsilon_c$) comes from a numerical solution of the Usadel equation while the high-temperature part comes from Eq. 1. From this figure, we can see that the characteristic decay temperature for the critical current is a few times the Thouless temperature ϵ_c/k_B . As soon as $k_B T > 5\epsilon_c$, the sum in Eq. (1) can be reduced to the first frequency term within a 3% underestimation. This term corresponds to $\omega_0 = \pi k_B T$ and $L_{\omega_0} = L_T$. Adding the second term in the summation decreases the error below 0.1% in the same temperature range.

The universal curve of Fig. 2 for $\Delta/\epsilon_c \rightarrow \infty$ is valid only in the case of a very long junction with $\Delta/\epsilon_c \gg 100$. It appears as if Δ is to be compared to the quantity $eR_N I_c(T=0) \simeq 10\epsilon_c$ in the long junction limit. In the limit of infinite Δ/ϵ_c , Eq. 1 simplifies to

$$eR_N I_c = \frac{32}{3 + 2\sqrt{2}} \epsilon_c \left[\frac{L}{L_T} \right]^3 e^{-L/L_T}. \quad (3)$$

From Eq. 3, one can get the temperature dependence of the critical current : $I_c \propto T^{3/2} \exp(-L/L_T)$. It has been demonstrated in Ref. [11] that within a limited temperature interval this expression is *numerically* very close to a simple exponential dependence $I_c \propto \exp(-L/L_T)$ with $L_T \propto 1/T$, as one would expect in a ballistic limit.^{23,24} From Fig. 2, the quasi-exponential temperature dependence of the critical current is indeed striking. This was the central result of Ref. [10], but was not understood at that time. This coincidence is purely accidental and has no special meaning.¹¹ In the low temperature limit, the numerical solution can be approximated by $eR_N I_c/\epsilon_c = a(1 - be^{-a\epsilon_c/3.2k_B T})$. The coefficients a and b are 10.82 and 1.30 respectively in the long junction limit $\Delta/\epsilon_c \rightarrow \infty$.

S-N-S junctions are intrinsically shunted and have negligible internal capacitance, so they are strongly overdamped. Their current-voltage characteristics are hence intrinsically non-hysteretic. The transition from a supercurrent to a voltage state happens at the critical current, but is rounded by finite temperature.²⁷ We fabricated Nb-Cu-Nb junctions²⁸ with a large conductance so that thermal fluctuations remain small compared to the Josephson energy : $k_B T \ll \hbar I_c(T)/2e$ even at high temperature near the critical temperature of Nb. This makes a well-defined critical current up to the critical temperature of Nb. Effects of environmental fluctuations known from mesoscopic tunnel junctions,²⁹ which are intrinsically underdamped, are absent.

We benefited from a trilayer stencil mask technology³⁰ making use of a thermostable resist that does not outgas during Nb evaporation. Thus we were able to routinely obtain a superconducting critical temperature as high as 8.1 K for the Nb electrodes. We performed successive shadow evaporations of Cu and Nb at different angles through the silicon stencil layer in an ultra high vacuum chamber, followed by a lift-off. Fig. 3 shows a typical sample. We studied a single sample (a) plus five different

samples evaporated on the same substrate (b, c, d, e and f). Table 1 lists the main physical parameters for these samples. The Cu metallic strips are 600 nm wide and 100 nm thick. The Nb superconducting electrodes are 800 nm wide and 200 nm thick, except for sample a where it is 100 nm. The length L of the metallic island was varied between 700 and 1000 nm, corresponding to a separation length d_{Nb} between Nb electrodes varying between 370 and 700 nm. For all samples, the calculated Thouless energy $\hbar D/L^2$ is therefore significantly smaller than the gap Δ .

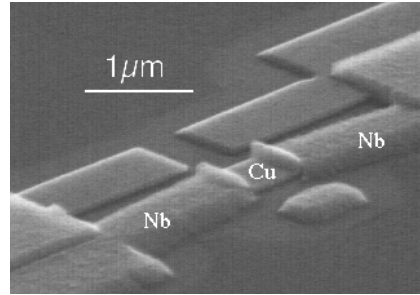


FIG. 3. Oblique micrograph of a typical S-N-S junction made of a Cu wire embedded between two Nb electrodes. The doubling of every structure due to the shadow evaporation is visible. The Nb electrodes cover the Cu strip over about 150 nm.

The normal-state resistance R_N cannot be directly measured at temperature above T_c since the resistance of the Nb electrodes is measured in series. We found that the finite-bias resistance ($eV \simeq \epsilon_c$) varied by about 10% between 2 K and 8 K due to the proximity effect on the conductance. We took for the normal-state resistance R_N the resistance at $T = 6 K$ for a better agreement with the theory. It is a relatively high temperature since $k_B T > 15\epsilon_c$ for every sample. Using L for the Cu length, we obtain a Cu resistivity $\rho = 1.1 \cdot 10^{-8} \Omega \cdot m$ for samples b to f and $\rho = 1.5 \cdot 10^{-8} \Omega \cdot m$ for sample a.

We measured the critical current of samples a to f at temperatures down to 300 mK. Our procedure consists in sweeping the bias current while measuring the differential resistance dV/dI . We define the experimental critical current as the current where the differential resistance reaches $R_N/2$. With this criteria, the experimental uncertainty is estimated below 0.5% at $T = 2 K$, 5% around $T = 4 K$ and 100% at 7 K. Fig. 4 shows the data for 3 samples. The measured $eR_N I_c/\epsilon_c$ plotted as a function of the reduced temperature $k_B T/\epsilon_c$ show a large decrease over more than two decades. For each sample, we fitted the data to the theoretical prediction with only one fitting parameter, the Thouless energy. The zero-temperature superconducting gap Δ was calculated from the measured critical temperature of Nb using : $\Delta = 3.8 k_B T_c$.³¹ This gives 1.3 meV for all samples except sample a for which $\Delta = 1 meV$. We used both a fixed gap equal to the zero-temperature value and a gap

$\Delta(T)$ following the BCS temperature dependence, but with a slightly reduced critical temperature $T_c = 7.5 K$. At high temperature, it appeared necessary to take into account the temperature dependence of the gap. In this case, the agreement between theory and experiment is excellent. The fit is very sensitive to the chosen value of the Thouless energy. We would like to stress that for each sample the horizontal and vertical axis are normalized to *the same* Thouless energy ϵ_c . This fitted values are found to be very close to the Thouless energies calculated from the full length L of the Cu strip, see Table I.

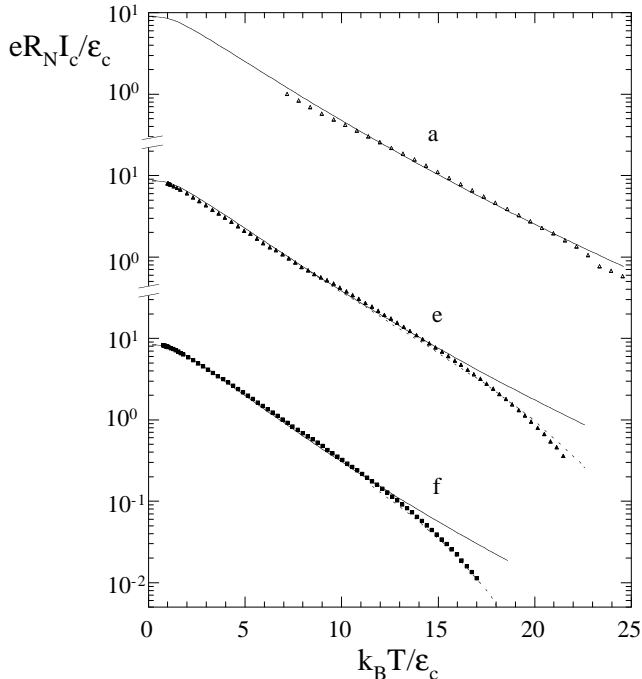


FIG. 4. Temperature dependence of the measured $eR_N I_c$ product of samples a, e and f together with the theoretical fits assuming a temperature-independent gap (full line) and a gap following a BCS temperature dependence with $T_c = 7.5 K$ (dashed line). The only adjustment parameter is the Thouless energy ϵ_c of each sample. For description of the sample parameters, see Table 1.

In Fig. 4, the critical current of sample f shows the onset of the saturation regime. At $T = 300mK$ the adjusted critical current $eR_N I_c$ reaches up to $8.2\epsilon_c$. This number is close to the theoretical value $8.79\epsilon_c$ for sample f at $T = 0$. This result discards an interpretation of our data within the Ginzburg-Landau theory of Ref. 12 which predicts a maximum $eR_N I_c / \epsilon_c$ of about 1.

In Ref. 10, an array of S-N-S junctions was made of a long N-metal wire periodically in contact with a series of superconducting islands. A good fit between the data and the theory was shown in Ref. [11], but with the introduction of a strong reduction of the effective area. This may be attributed to the periodic and lateral characters of this type of samples.

Our calculation assumes perfectly transmitting inter-

faces with zero boundary resistance. In fact, it is sufficient that the barrier-equivalent length³² $L_t = l_c/t$ is much smaller than the sample length. As an example, this condition means an interface transparency $t > 0.1$ for sample b. In the case of Nb-Cu-Nb samples fabricated through a two-lithography-step process including Ar-etching,³³ we found a critical current with a reduced magnitude, presumably due to a slightly degraded interface. The critical current in S-N-S junctions with partially transparent interfaces was discussed in Ref. [34]. The predicted behavior features a different temperature dependence for the critical current. Nevertheless, the temperature dependence remained consistent with the theory assuming a perfect interface. Only a reduction prefactor had to be introduced. This observation could hint at the fact, that interface barriers are very inhomogenous and the current is carried through a few highly conducting pinholes.

In summary, we discussed the Josephson critical current of diffusive S-N-S junctions. This study provides a simple and reliable formulation that enables the practical determination of the equilibrium critical current. We studied the critical current of a set of samples with different junction lengths and found an excellent agreement between our data and the predictions of the quasiclassical theory.

We acknowledge discussion and financial support in the EU-TMR network "Dynamics of superconducting circuits" as well as support from the DFG through SFB 195 and GK 284. We thank A. Golubov, T.T. Heikkilä, D. Mailly, N. Moussy and P. Paniez for discussions.

-
- ¹ J. Clarke, *Proc. Roy. Soc. A* **308**, 447 (1969).
 - ² J. G. Shepherd, *Proc. Roy. Soc. A* **326**, 421 (1972).
 - ³ P. G. de Gennes, *Rev. Mod. Phys.* **36**, 225 (1964).
 - ⁴ H. J. Fink, *Phys. Rev. B* **14**, 1028 (1976).
 - ⁵ J. Warlaumont, J. C. Brown and R. A. Buhrman, *Appl. Phys. Lett.* **34**, 415 (1979).
 - ⁶ R. B. van Dover, A. de Lozanne and M. R. Beasley, *J. Appl. Phys.* **52**, 7327 (1981).
 - ⁷ K. K. Likharev, *Sov. Tech. Phys. Lett.* **2**, 12 (1976).
 - ⁸ K. D. Usadel, *Phys. Rev. Lett.* **25**, 507 (1970).
 - ⁹ A. D. Zaikin and G. F. Zharkov, *Sov. J. Low Temp. Phys.* **7**, 184 (1981). In Eq. 14 and 15 of that paper, the prefactor 128 refers to the case where R_N is the resistance *per spin*. It should be replaced by 64 if one identifies R_N with the full resistance.
 - ¹⁰ H. Courtois, Ph. Gandit and B. Pannetier, *Phys. Rev. B* **52**, 1162 (1995).
 - ¹¹ F. K. Wilhelm, A. D. Zaikin and G. Schön, *J. of Low Temp. Phys.* **106**, 305 (1997).
 - ¹² H. J. Fink, *Phys. Rev. B* **56**, 2732 (1997).
 - ¹³ see the special issue of *Superlattices and Microstructures*,

Vol. 25, No. 5/6 (1999).

- ¹⁴ H. Courtois, Ph. Gandit, D. Mailly and B. Pannetier, *Phys. Rev. Lett.* **76**, 130 (1996).
- ¹⁵ B. Pannetier and H. Courtois, *J. of Low Temp. Phys.* **118**, 599 (2000).
- ¹⁶ J. J. A. Baselmans, A.F Morpurgo, B. J. van Wees, T. M Klapwijk, *Nature* **397**, 43 (1999).
- ¹⁷ F. K. Wilhelm, G. Schön and A. D. Zaikin, *Phys. Rev. Lett.* **81**, 1682 (1998).
- ¹⁸ J. Kutchinsky, R. Taboryski, C. B. Sørensen, J. B. Hansen and P. E. Lindelof, *Phys. Rev. Lett.* **83**, 4856 (1999).
- ¹⁹ W. Belzig, F. K. Wilhelm, C. Bruder, G. Schön and A.D. Zaikin, in Ref.¹³. (1985).
- ²⁰ K. A. Delin and A. W. Kleinsasser, *Supercond. Sci. Technol.* **9**, 227 (1996).
- ²¹ In the long junction regime $\Delta > \epsilon_c$, the extrapolation of low¹¹ or high¹² energy dependencies provides a reasonable parameter dependence, but fails to predict the correct prefactor.
- ²² A. Yu. Kasumov *et al.*, *Science* **284**, 1508 (1999).
- ²³ I. O. Kulik, *Sov. Phys. JETP* **30**, 944 (1970).
- ²⁴ C. Ishii, *Progr. Theor. Phys.* **14**, 1525 (1970).
- ²⁵ I. O. Kulik and A. N. Omel'yanchuk, *Sov. J. Low Temp. Phys.* **4**, 142 (1978).
- ²⁶ A. D. Zaikin and S. V. Panyukov, *Sov Phys. JETP* **62**, 137 (1985).
- ²⁷ V. Ambegaokar and B. I. Halperin, *Phys. Rev. Lett.* **22**, 1364 (1969).
- ²⁸ F. K. Wilhelm, G. Schön, A. D. Zaikin, A. A. Golubov, P. Dubos, H. Courtois, and B. Pannetier, *Physica B* **284-288** 1836 (2000)
- ²⁹ D. Vion, M. Götz, P. Joyez, D. Estève and M. H. Devoret, *Phys. Rev. Lett.* **77**, 3435 (1996).
- ³⁰ P. Dubos, P. Charlat, Th. Crozes, P. Paniez and B. Pannetier, *J. Vac. Sci. Technol. B* **18**, 122 (2000).
- ³¹ N. Ashcroft and N. Mermin, *Solid State Physics*, Holt-Saunders Ed. (1976).
- ³² F. Zhou, B. Spivak, and A. Zyuzin, *Phys. Rev. B* **52**, 4467 (1995).
- ³³ P. Dubos and D. Mailly, unpublished.
- ³⁴ M. Yu. Kuprianov and V. F. Lukichev, *Sov. Phys. JETP* **67**, 1163 (1988).

#	L (nm)	d_{Nb} (nm)	w (nm)	$R_{\text{N},6\text{K}}$ (Ω)	D (cm^2/s)	$\hbar D/L^2$ (μeV)	ϵ_c (μeV)	Δ/ϵ_c	$\frac{eR_{\text{N}}I_G}{\epsilon_c}(T=0)$
a	1000	600	600	0.260	200	13	14.3	70	8.91
b	1010	680	580	0.173	300	20	18.6	70	8.99
c	910	570	590	0.179	260	22	21.7	60	8.83
d	800	470	580	0.183	230	25	25.4	51	8.64
e	800	476	590	0.169	250	26	26.1	50	8.62
f	710	370	580	0.152	250	34	33.5	39	8.32

TABLE I. Parameters of the different samples studied. L is the full length of Cu strip while d_{Nb} is the Nb electrodes separation. w is the Cu strip width. The Thouless energy ϵ_c is derived from the fit of the experimental data to the theoretical prediction (see Fig. 4).